Plasticizing Li Single-ion Conductors with Low-Volatility Siloxane Copolymers and Oligomers Containing Ethylene Oxide and Cyclic Carbonates

Journal:	*Journal of Materials Chemistry A*
Manuscript ID:	TA-ART-08-2015-006042.R1
Article Type:	Paper
Date Submitted by the Author:	08-Sep-2015
Complete List of Authors:	Liang, Siwei; Lawrence Berkeley National Lab, Materials Science Devision Chen, Quan; Pennsylvania State University, Materials Science and Engineering Choi, U; Pennsylvania State University, Materials Science and Engineering bartels, Josh; Pennsylvania State University, Materials Science and Engineering; Pennsylvania State University, Materials Science and Engineering Bao, Nanqi; Pennsylvania State University, Materials Science and Engineering Runt, James; Pennsylvania State University, Materials Science and Engineering Colby, Ralph H. ; Pennsylvania State University, Materials Science and Engineering

Plasticizing Li Single-ion Conductors with Low-Volatility Siloxane Copolymers and Oligomers Containing Ethylene Oxide and Cyclic Carbonates

Siwei Liang,[1,2] *Quan Chen,*[1,3†] *U Hyeok Choi,*[1,4] *Joshua Bartels,*[1] *Nanqi Bao,*[1] *James Runt,*[1] *and Ralph H. Colby*[*1]

1. Materials Science and Engineering,
The Pennsylvania State University, University Park, PA 16802
2. Joint Center for Artificial Photosynthesis, Lawrence Berkeley National Laboratory,
One Cyclotron Road, Berkeley, CA 94720
3. State Key Laboratory of Polymer Physics and Chemistry, Changchun Institute of Applied Chemistry,
Chinese Academy of Sciences, Changchun 130022, People's Republic of China
4. Functional Composites Department, Korea Institute of Materials Science, Changwon, 642-831, Korea

Abstract

To prepare safe electrolyte for lithium ion batteries, two groups of novel low-volatility plasticizers combining pendant cyclic carbonates and short ethylene oxide chains have been successfully synthesized, as confirmed by ^{1}H and ^{29}Si NMR spectroscopy. The Fox equation describes the composition dependence of the glass transition temperature (T_g) very well for the random polysiloxane-based copolymer plasticizers (with $10000 < M < 13000$) while the smaller oligomer plasticizers have T_g as much as 20 K lower than the Fox equation prediction because of their lower molecular weight ($300 < M < 700$). The Landau-Lifshitz mixing rule describes the dielectric constant of the random polysiloxane-based copolymer plasticizers at all temperatures above T_g. Mixing with 20wt% polysiloxane tetraphenyl borate – Li ionomer (14 mol% borate and 86 mol% cyclic carbonate) increases conductivity relative to the neat ionomer by lowering T_g, increasing dielectric constant and providing better solvation of Li$^+$. The best oligomeric plasticizer only has T_g 10 K lower than the Fox prediction but has dielectric constant 30% larger than expected by the Landau-Lifshitz mixing rule, owing to a surprisingly low viscosity, resulting in ambient conductivity 2×10^{-5} S/cm. For both groups of plasticizers, the fraction of cyclic carbonates relative to ethylene oxide governs the magnitude and temperature dependence of the ionic conductivity.

---

† co-first author

* email to: rhc@plmsc.psu.edu

Introduction

Polymer electrolytes as energy materials are of great interest for lithium-ion battery, fuel cell, solar cell and actuator applications, due to the inherent polymeric merits, such as mechanical robustness and ease of processing to make thin-film membranes. Among different types of polymer electrolytes, single-ion conductors with one type of ion covalently bonded to the polymer have recently attracted increased attention, owing to (1) high selectivity of conducting ions (lithium ion transference number near unity) and (2) elimination of anion polarization at the electrode/electrolyte interface that weakens the electric field inside the electrolyte and causes safety problems.[1-6]

Ionomers with weak binding borate anions are particularly useful as cation conductors.[7-10] Since the boron is less electronegative than carbon, B is positive and the negative charge is delocalized, weakening the ion pair energy with Li^+ and other cations.[11, 12] Recently developed novel tetraphenyl borate – Li polysiloxane single-ion conductors[13] with cyclic carbonate side chains were shown to have exceptionally low conducting ion activation energy (7-10 kJ/mol) from the weak binding between delocalized anions and Li^+ and the strong solvation of Li^+ from the carbonate oxygens. The nonionic polysiloxane homopolymer with only cyclic carbonate side chains has dielectric constant ~50 near room temperature, further weakening the ionic interactions. However, it seems that the large tetraphenyl borate anions repel the cyclic carbonate side chains, effectively aggregating the ions on the nanoscale, which raises T_g, lowers segmental mobility, and traps the majority of the Li^+ ions in aggregates, with only between 1% and 5% of the Li^+ ever participating in conduction, as seen in the infinite temperature intercept of the Arrhenius simultaneously conducting Li^+ content.[13]

Addition of polar solvating plasticizers can improve the conductivity through three effects: (1) lowering T_g to improve ionic mobility, (2) raising dielectric constant to weaken the ionic interactions and (3) providing specific solvation of Li^+, with the former one to enhance ionic mobility and the latter two to increase participation of Li^+ in conduction. By simply crosslinking, the polyelectrolytes swollen in polar solvating plasticizers, one makes so-called gel electrolytes.[14-19] When mixing with single-ion conductors, plasticizers appear to solvate and transport Li^+ cations more efficiently. In particular, cyclic carbonates such as propylene carbonate (PC) and ethylene carbonate (EC) have been widely used as plasticizers in the Li-ion battery industry, due to their high dielectric constant, strong solvation of Li^+ and ability to form a stable electrode-electrolyte interfacial layer. However, safety issues caused by leakage and evaporation of these small-molecule carbonates prompt scientists to pursue non-volatile alternatives. Poly(ethylene glycol) (PEG) is considered as a good candidate because it can break ion aggregates and solvate cations: When Li^+ leaves an ion aggregate, the ether oxygen of PEG can solvate and stabilize the free Li^+.[20-28] Recently, PEG with molecular weight of 600 g/mol has been shown to greatly enhance conductivity of siloxane tetraphenyl borate Li single-ion conductors with cyclic carbonate side chains;[22] although crystallization of the PEG oligomers near room temperature led to an abrupt drop in conductivity at lower temperatures when more than ~40 wt% PEG was added.

This paper explores novel plasticizers of low-volatility at working conditions of lithium-ion batteries. They are composed of ether-oxygen units (low T_g, moderate polarity and strong specific solvation of Li^+) and cyclic carbonate units (higher T_g, higher polarity and similar strong solvation of Li^+) with molecular weight $300 < M < 12000$. The composition of the low-volatility plasticizers was carefully tuned. Blends of these plasticizers with 20 wt% of a tetraphenyl borate

– Li polysiloxane single-ion conductor chains exhibit improved ionic conductivity up to 2x 10^{-5} S/cm at 25 ºC. Furthermore, all the plasticizers and their mixtures are strictly amorphous, allowing a wider temperature range for applications.

Experimental

Materials. Dichloromethane, diethyl carbonate, chlorodimethylsilane, triethyl amine (NEt_3), tetraethylene glycol, potassium carbonate, 2-(2-vinyloxy) ethoxy) ethanol, diethyl carbonate, toluene and anhydrous acetonitrile were purchased from VWR and used without further purification. Platinum divinyltetramethyldisiloxane complex (Pt[dvs]) (3% in xylene) catalyst, diethyldihydrosilane, tri(ethylene glycol) divinyl ether, di(ethylene glycol) divinyl ether, $RhCl(PPh_3)_3$ catalyst and polymethylhydrosiloxane (PMHS, M_n = 1700 - 3200) were purchased from Aldrich and used as received. Tetrahydrofuran (THF) from EMD Chemicals was refluxed over sodium metal before use. The polysiloxane-based ionomer was prepared by the method reported in ref. 3 with ion contents of 14 mol%.

Characterization. *^{1}H, ^{13}C and ^{29}Si NMR spectroscopy* were recorded on a Bruker AM 300M spectrometer. Glass transition temperatures (T_g) were determined using a TA Q100 *differential scanning calorimeter (DSC)* at 10 K/min heating and cooling rates. *Dielectric relaxation spectroscopy (DRS)* measurements were conducted on samples sandwiched between two polished brass electrodes, with 50 μm silica spacers placed in between the two electrodes. The sandwiched samples were positioned in a Novocontrol GmbH Concept 40 broadband dielectric spectrometer and the dielectric permittivity and conductivity were measured using an AC voltage amplitude of 0.1 V and 10^{-2}-10^{7} Hz frequency range. Prior to the DRS measurements, the samples were annealed in the Novocontrol at 120°C in a heated stream of dry nitrogen for 1 hour to drive off any moisture picked up during loading of these hygroscopic materials. Data were collected in isothermal frequency sweeps from 120°C to near T_g. *Linear viscoelastic measurements* were conducted with Advanced Rheometric Expansion System (ARES-LS, Rheometric Scientific). Parallel plates with diameters of 25mm, were utilized to conduct dynamic frequency sweeps at room temperature (21°C). Strain amplitudes lower than 0.1 were applied and confirmed to be in the linear response region.

Cyclic [(allyloxy) methyl] ethylene ester carbonic acid (CECA). CECA was prepared according to the method reported in ref. 13. Potassium carbonate (3 g, 21.7 mmol) was added to a mixture of 3-(allyloxy)-propane-1, 2-diol (92.4 g, 0.188 mol) and diethyl carbonate (24.8 g, 0.188 mol). After stirring at 120 °C for 24h, the mixture was filtered to isolate the solid. The residue was purified by Kügelrohr distillation to yield the pure product as a colorless liquid (23.7 g, 80%). ^{1}H NMR (in $CDCl_3$), δ(ppm) 5.87 (m, 1H, C=CH), 5.25 (d, 1H, cis H of CH_2=C), 5.14 (d, 1H, trans H of CH_2=C), 4.86 (m, 1H, CCH(C)O), 4.38-4.55(m, 2H, CH_2C), 4.06 (m, 2H, OCH_2C=C), 3.60-3.74 (m, 2H, $OCCH_2O$).

Tri(ethylene glycol) allyl methyl ether (Vinyl PEO_3). Vinyl PEO_3 was prepared according to literature method. To a mixture of NaH (1.44g, 60% in mineral oil) dispersed in 20 mL dry THF was added solution of tri(ethylene glycol) methyl ether (4.7 mL, 0.03 mol) in 150mL of THF dropwise at ice-bath temperature. The mixture was stirred for 3 hours before being transferred into a solution of allyl bromide (3.58g, 0.03mol) in 20 mL dry THF. The mixture was allowed to react overnight to complete the reaction. The reaction was quenched by ice water and extracted by ethyl acetate (20 mL x 3). The organic phases were combined and condensed by rotavap. The yellowish liquid was then purified by vacuum distillation to yield (5.5 g, 90%). ^{1}H NMR (in d6-

acetone), δ(ppm) 5.85(m, 1H, CH=), 5.2 (s, (d, cist H of = CH_2), 5.1 (d, trans H of = CH_2), 3.95 (d, 2H, $C{=}CCH_2$), 3.8-3.6 (m, 8H, OCH_2CH_2O), 3.35 (s, CH_3).

General procedure for synthesis of polymer plasticizers CPP(0, 19 31, 57, 80, 100). PMHS was added into a pre-dried flask equipped with a condenser. The desired amount of CECA and vinyl PEO_3 were charged into the flask followed by 20 mL anhydrous CH_3CN and 0.2 mL Pt catalyst. The reaction mixture was stirred at 70 ºC. The completion of the reaction was confirmed by ^1H NMR. The reaction time was in the range of 2-7 days. The mixture was condensed and the residue was dissolved in toluene and precipitated in hexane 3 times. Afterwards, the product was dried in a vacuum oven at 80 ºC for 24 hours.

4,4'-(6,6,21,21-tetramethyl-2,7,10,13,16,19,25-heptaoxa-6,21-disilahexacosane-1,26-diyl)bis (1,3-dioxolan-2-one) (**OP62**) CECA (10.86g, 0.068mol), anhydrous CH_3CN (20mL) and chlorodimethylsilane (7.67g, 0.081mol) were added into a pre-dried flask. The mixture was cooled by icebath before 0.3 ml Pt catalyst was charged. The mixture was allowed to react overnight to complete the reaction. The solvent was evaporated and the residue was vacuum distilled to obtain 4-((3-(chlorodimethylsilyl)propoxy)methyl)-1,3-dioxolan-2-one as a colorless liquid (15.2g, 89%). ^1H NMR (in d6-acetone), δ(ppm) 4.95 (m, 1H, CCH(C)O), 4.4-4.6(m, 2H, CH_2C), 3.75 (m, 2H, $CC\underline{H}_2OCH2CH_2H_2$), 3.55 (m, 2H, $OC\underline{H}_2CH_2CH_2$), 1.7 (m, 2H, $OCH_2C\underline{H}_2CH_2$), 0.9 (m, 2H, $OCH_2CH_2C\underline{H}_2$), 0.35 (m. CH_3); ^{29}Si NMR (in d6-acetone) 33 (s); (**Figure S2**) ^{13}C NMR (in d6-acetone), δ(ppm) 160, 75.1, 74.8, 74, 73.2, 23, 15, 0.2. (**Figure S3**)

4-((3-(chlorodimethylsilyl)propoxy)methyl)-1,3-dioxolan-2-one (8.7g, 0.034 mol) was added dropwise into the mixture of NEt_3 (7.5g), tetraethylene glycol (6.67g, 0.034mol) and 20 mL dry THF over 30 minutes. The reaction mixture was allowed to stir overnight to complete the reaction. The mixture was filtered to remove solid. The liquid was condensed by rotavap and further dried by vacuum oven to yield OP62 as a brown liquid (13g**).** ^1H NMR (in d6-acetone), 4.95 (m, 1H, CCH(C)O), 4.4-4.6(m, 2H, CH_2C), 3.75 (m, 2H, $CC\underline{H}_2OCH_2CH_2H_2$), 3.63 (s, 16 H, OCH_2CH_2O) 3.55 (m, 2H, $OC\underline{H}_2CH_2CH_2$), 1.7 (m, 2H, $OCH_2C\underline{H}_2CH_2$), 0.9 (m, 2H, $OCH_2CH_2C\underline{H}_2$), 0.35 (m. CH_3); ^{29}Si NMR (in d6-acetone) 17.57 (s). (**Figure S4**)

4,4'-(6,6,22,22-tetraethyl-2,9,12,15,19,26-hexaoxa-6,22-disilaheptacosane-1,27-diyl)bis(1,3-dioxolan-2-one) (OP73) Diethyldihydrosilane (7.2g, 0.082 mol), CECA (8.4g, 0.053 mol) and 10 mL benzene were added into flask followed by 0.1g $RhCl(PPh_3)_3$ catalyst. The mixture was stirred at room temperature overnight to complete the reaction. The solvent was evaporated and the residue was vacuum distilled to afford 4-((3-(diethylsilyl)propoxy)methyl)-1,3-dioxolan-2-one as a colorless liquid (20g, 100%). ^1H NMR (in d6-acetone), 4.95 (m, 1H, CCH(C)O), 4.4-4.6(m, 2H, CH_2C), 3.45 to 3.8 (m, 5H, $CC\underline{H}_2OCH_2CH_2CH_2$, $OC\underline{H}_2CH_2CH_2$ and SiH), 1.64 (m, 4H, $OCH_2C\underline{H}2CH_2Si$), 1 (m, 6H, $OCH_2CH_2C\underline{H}_2$ and $SiCH_2$), 0.67 (m, 6H, CH_3); ^{29}Si NMR (in d6-acetone) -1.38 (s). (**Figure S5**)

4-((3-(diethylsilyl)propoxy)methyl)-1,3-dioxolan-2-one (5g, 0.02 mol) and tri(ethylene glycol) divinyl ether (2g, 0.01mol) were mixed followed by 0.1g $RhCl(PPh_3)_3$ catalyst. The mixture was stirred at room temperature overnight to complete the reaction. The solvent was evaporated and the residue was washed by heptanes to afford product as a brown liquid (7g). ^1H NMR (in d6-acetone), 4.95 (m, 1H, CCH(C)O), 4.4-4.6(m, 2H, CH_2C), 3.45 to 3.8 (m, 12H, $CC\underline{H}_2OCH_2CH_2CH_2$, $OC\underline{H}_2CH_2CH_2$ and OCH_2CH_2O), 1.64 (m, 4H, $OCH_2C\underline{H}_2CH_2Si$), 1 (m, 6H, $OCH_2CH_2C\underline{H}_2$ and $SiCH_2$), 0.67 (m, 6H, CH_3); ^{29}Si NMR (in d6-acetone) 5.25 (s). (**Figure S6**)

4,4'-(6,6,20,20-tetraethyl-2,9,13,17,24-pentaoxa-6,20-disilapentacosane-1,25-diyl)bis(1,3-dioxolan-2-one) (OP67). The same procedure as synthesis of OP73 was used with di(ethylene glycol) divinyl ether as a linker. ^{1}H NMR (in d6-acetone), 4.95 (m, 1H, CCH(C)O), 4.4-4.6(m, 2H, CH_2C), 3.45 to 3.8 (m, 10H, $C\underline{H_2}OCH_2CH_2CH_2$, $O\underline{CH_2}CH_2CH_2$ and OCH_2CH_2O), 1.64 (m, 4H, $OCH_2C\underline{H_2}CH_2Si$), 1 (m, 6H, $OCH_2CH_2C\underline{H_2}$ and $SiCH_2$), 0.67 (m, 6H, CH_3) (**Figure S7**)

Results and Discussion

Synthesis

Two types of plasticizers were synthesized. The first type is copolymerized plasticizer (CPP), having $(EO)_3$ side chains and cyclic carbonate side chains, synthesized by hydrosilylation using a method described in our previous work (**Scheme 1**).[13] The CPP samples are coded according to the fraction *f* of carbonate-containing units, as determined by the integrated areas of ^{1}H NMR peaks (see Figure S1 and Table S1 for details). For example, CPP-19 means copolymerized plasticizer having molar fraction *f* = 19% of carbonate containing units.

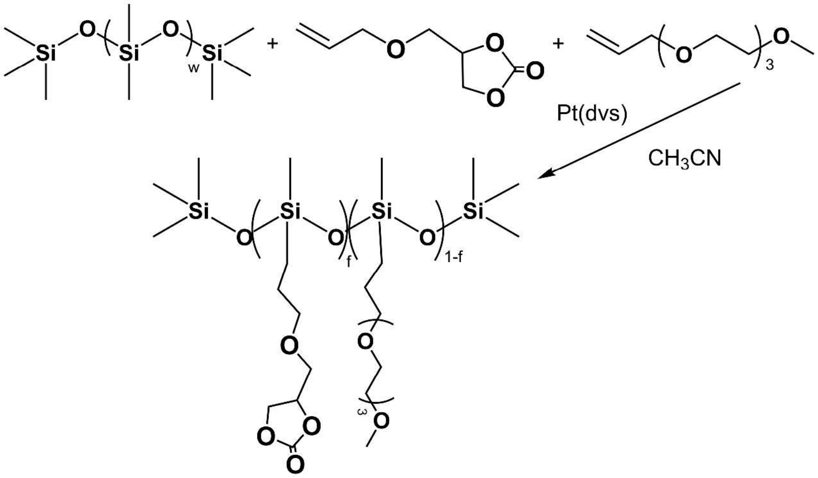

Scheme 1. Synthesis of siloxane random copolymer plasticizers CPP-(0, 19, 31, 57, 80, 100), where the number is the mol% of cyclic carbonate containing units, i.e., 100*f*.

To further improve the performance of the low-volatility plasticizers, the second type of oligomeric plasticizers (OP) of $300 < M < 700$ were synthesized by condensation reactions (**Scheme 2**). To better compare with the CPP, an equivalent f' is calculated based on the carbonate:EO ratio. Since the CPPs have carbonate side chain (with one cyclic carbonate group and one EO) and EO side chain (with four EOs), the ratio of carbonate:EO $= f/[f+4(1-f)]$. For OP, by allowing carbonate:EO $= f'/[f'+4(1-f')]$ enables an estimation of f' analogous to f of CPP. OPs are coded according to f', for example OP73 means $f' = 73\%$.

OP-62 was synthesized by condensation reaction with triethyl amine as acid scavenger (Scheme 2(a)). The resulting product with Si-O-C linkages is moisture sensitive. The first attempt to synthesize OP67 and OP73 (Scheme 2(b)) failed because the platinum catalyst that works for most of hydrosilylation reactions gave nearly no desired product. Well-known Wilkinson Rh catalyst [$RhCl(PPh_3)_3$] suggested by Hartwig et al. exhibited better catalyzing capability.[29] The hydrosilylation for the second SiH groups on the same Si atom didn't start until all the first SiH groups were consumed, as confirmed by ^1H NMR. The synthesis of OP-89 (Scheme 2(c)) is straightforward. The reaction was impossible to stop at the monosubstitution state, even with excess dihydrosilane.

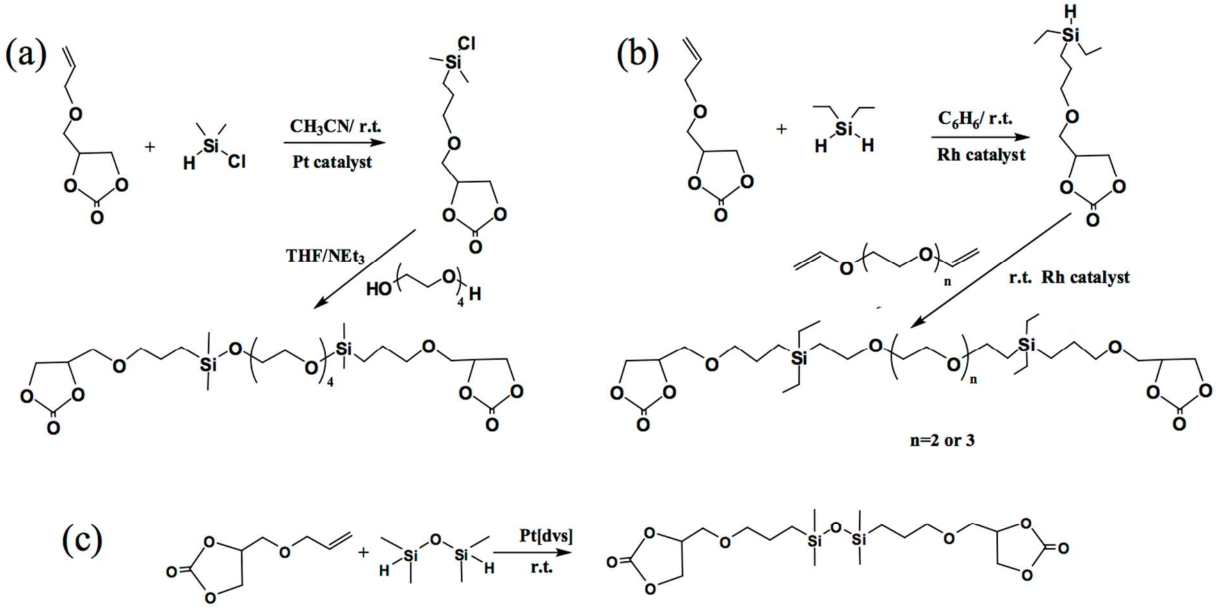

Scheme 2. Synthesis of oligomer plasticizers (a) OP62, (b) OP73 (n=2) and OP67 (n=3), and (c) OP89.

The OP and CPP samples were blended with a tetraphenyl borate – Li polysiloxane single-ion conductor synthesized in our previous work, having 14 mol% tetraphenyl borate-86 mol% cyclic carbonate ionomer with Li^+ counterions.[13] The weight fraction of ionomer in all mixtures is w = 20wt%. To prepare the mixtures, the ionomer and plasticizer were dissolved in a common solvent acetone and the solvent was evaporated first via rotovap and then the blends were put in vacuum oven at 80 ºC. Since OP evaporates slowly in vacuum at 80 ºC, 5~10wt% extra OP was added in the common solvent, and the sample was weighed every 2-3 hours after introducing into the vacuum oven to record the weight loss of OP with time. More than 10 hours in vacuum oven was required to evaporate the extra OP and obtain the target content of 20wt% ionomer.

Glass Transition Temperature

Glass transition temperatures (T_g) of CPP and OP are plotted against f and f', respectively, in Figure 1 in filled symbols. T_g of CPP increases with polar carbonate content f. The overall trend is well predicted by the Fox equation (thick solid curve in Figure 1):

$$\frac{1}{T_g} = \frac{f}{T_{g,\text{CPP-100}}} + \frac{1-f}{T_{g,\text{CPP-0}}} \tag{1}$$

T_gs of OPs are lower than T_gs of CPPs and the Fox equation prediction. The Fox equation (1) can predict T_g of the random copolymers from those of the two homopolymers when the copolymer and homopolymers have (1) similar chain sizes and thus an effect of chain ends, known to cause extra free volume, have equal contribution to T_g, or (2) sufficiently large chain sizes and thus an effect of chain ends is negligible. Since OPs are oligomers for which chain ends play a big role in reducing T_g, the OPs having T_g well below the Fox equation of the much longer homopolymers is reasonable. This argument also explains the overall trend of T_g further below the Fox prediction at higher f': considering that each OP molecule contains identically two carbonate end groups, larger f' simply means shorter chain and accordingly stronger chain end effect. Blended with 20wt% ionomer with significantly higher T_g (=301 K), the mixtures display only ~5K higher T_g than the plasticizers alone. The increase is less than the Fox prediction of equation 2 shown as the dashed curve in Figure 1, suggesting that an ion-solvating effect lowers T_g, which is more obvious when EO units are present in the plasticizer.

$$\frac{1}{T_g} = \frac{w}{T_{g,\text{ionomer}}} + \frac{f(1-w)}{T_{g,\text{CPP-100}}} + \frac{(1-f)(1-w)}{T_{g,\text{CPP-0}}} \tag{2}$$

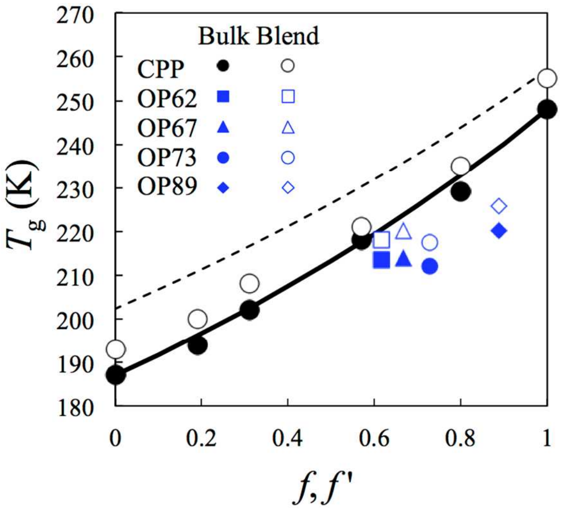

Figure 1. Plots of T_g of CPP and OP plasticizers against f and f', respectively (filled symbols). T_g of resulting blends (80wt% plasticizer and 20wt% ionomer) is added for comparison (open symbols). Thick solid and thin dashed curves show predictions of Fox equations 1 and 2, respectively.

Dielectric constant

In Figure 2a, the static dielectric constant ε_s of CPP increases with content of polar cyclic carbonate groups. The data of the four CPP random copolymers can be predicted from the two CPP homopolymers (CPP-100 and CPP-0) very well with Landau and Lifshitz's mixing rule,[30] at all temperatures in the liquid state (solid curves in Figure 2a).

$$\varepsilon_s^{1/3} = f\varepsilon_{s,\text{CPP-100}}^{1/3} + (1-f)\varepsilon_{s,\text{CPP-0}}^{1/3} \qquad (3)$$

While the CPP-0 homopolymer perfectly obeys the Onsager equation (dotted line in Figure 2a)[31] the CPP-100 homopolymer exhibits strong curvature for reasons that are not apparent, yet still the Landau-Lifshitz mixing rule works perfectly for all four random copolymers.

Figure 2(b) compares the static dielectric constants ε_s of the four OPs and CPPs, which are comparable when f' and f are comparable (compare OPs of f' = 62% to 89% to CPPs of f = 57% to 80% in Figure 2(b)). This feature is more clearly seen in the inset, where ε_s of CPPs and OPs at T = 20°C are plotted against f and f', respectively.

In comparison, ε_s of OPs scatters closely around the Landau and Lifshitz curve, meaning the dielectric constant for both OP is governed by the carbonate:EO ratio. The considerable scattering should be related to detailed molecular structure. Considering ε_s here reflects a response of the dipole moments to perturbed electric field, it should be related to not only the density of dipoles but also how the dipoles interact with each other, i.e. dipole-dipole correlation. The latter effect should rely on the molecular structure, in particular an energy barrier for dipole rotation. For example, OP62 has ε_s considerably higher than that expected from f'. The reason could be related to the ultra-flexible Si-O bond that allows the polar carbonate group to respond more easily to an applied electric field.[32-35] This argument is in accordance with the observation that OP62 and OP89 having Si-O bonds exhibit ε_s higher than those of CPPs, while OP67 and OP73 having no Si-O bond exhibit ε_s lower than those of the CPPs. The dielectric constants of the mixtures with 20wt% ionomer are shown in Figure 2(c), with blend dielectric constant increasing with cyclic carbonate content.

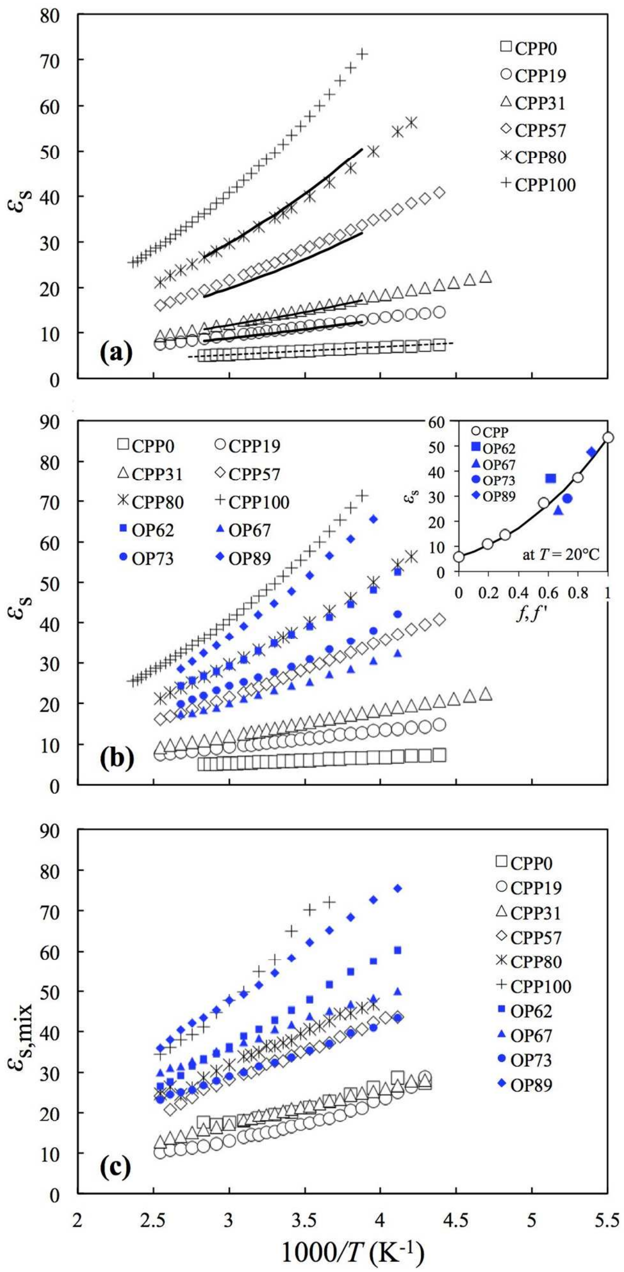

Figure 2. (a) Temperature dependences of static dielectric constant ε_s of CPPs (in symbols) and the predictions by the Landau and Lifshitz's mixing rule (eq 3, solid curves) and the Onsager equation (dotted line). (b) Comparison of dielectric constants of the CPPs (in black symbols) and OPs (in blue symbols). Inset: Static dielectric constant ε_s at T = 20°C increases with the fraction of carbonate units f for the six CPPs (open symbols). The solid curve is Landau and Lifshitz's mixing rule, eq. 3. ε_s vs f' of the four OPs are added for comparison (filled symbols). The significantly larger ε_s of OP62 seems to play a role in its superior conductivity. (c) Dielectric constant of mixtures of 20 wt% of 14 mol% lithium tetraphenyl borate / 86 mol% cyclic carbonate random copolymer ionomer[13] with 80 wt% of the various plasticizers.

Figure 3 (a) shows the temperature dependence of ionic conductivity σ_{DC} of the ionomer (red symbols) and its 20 wt% mixtures with CPP (black symbols) and OP (blue symbols). For CPP mixtures, the conductivity shows an interesting crossover, increasing with f at sufficiently high T while decreasing with f at sufficiently low T. This result reflects a tradeoff between reducing T_g via increasing the EO content and increasing ε_s via increasing the cyclic carbonate content, as explained earlier in Figures 1 and 2. The reduction of T_g (faster segmental motion) boosts ionic mobility and dominates at low T close to T_g. The increase of ε_s softens ionic interactions and facilitates ion dissociation; this effect dominates at high T, sufficiently far above T_g. The effect of ε_s increasing with cyclic carbonate content is more clearly seen in Figure 3(b) where temperature has been normalized by $T_{g.}$ At constant T_g/T, σ_{DC} increases with f for the CPP mixtures. This trend is also seen in the OP mixtures, the conductivity decreases in the order OP89 ~ OP62 > OP73 > OP67, in accordance with the order of their ε_s.

In Figure 3(a), σ_{DC} is larger for the OP mixtures than the CPP samples even if f and f' are comparable, reflecting the smaller OP molecules exhibit lower viscosity than the larger CPP molecules. The lower viscosity is due partly to the lower T_g for OPs seen in Figure 1, and also partly to the smaller size of the OPs. In accordance with this argument, the inset of Figure 3 (a) shows an overall trend that σ_{DC} increases with an inverse of zero-shear viscosity η_0 at $T = 20°\mathrm{C}$ (see Table 1), well-known as Walden's rule.[36] Figure 3(c) shows that dividing conductivity by the dielectric constant of the mixture does not quite reduce all data to a common curve plotted against T_g/T.

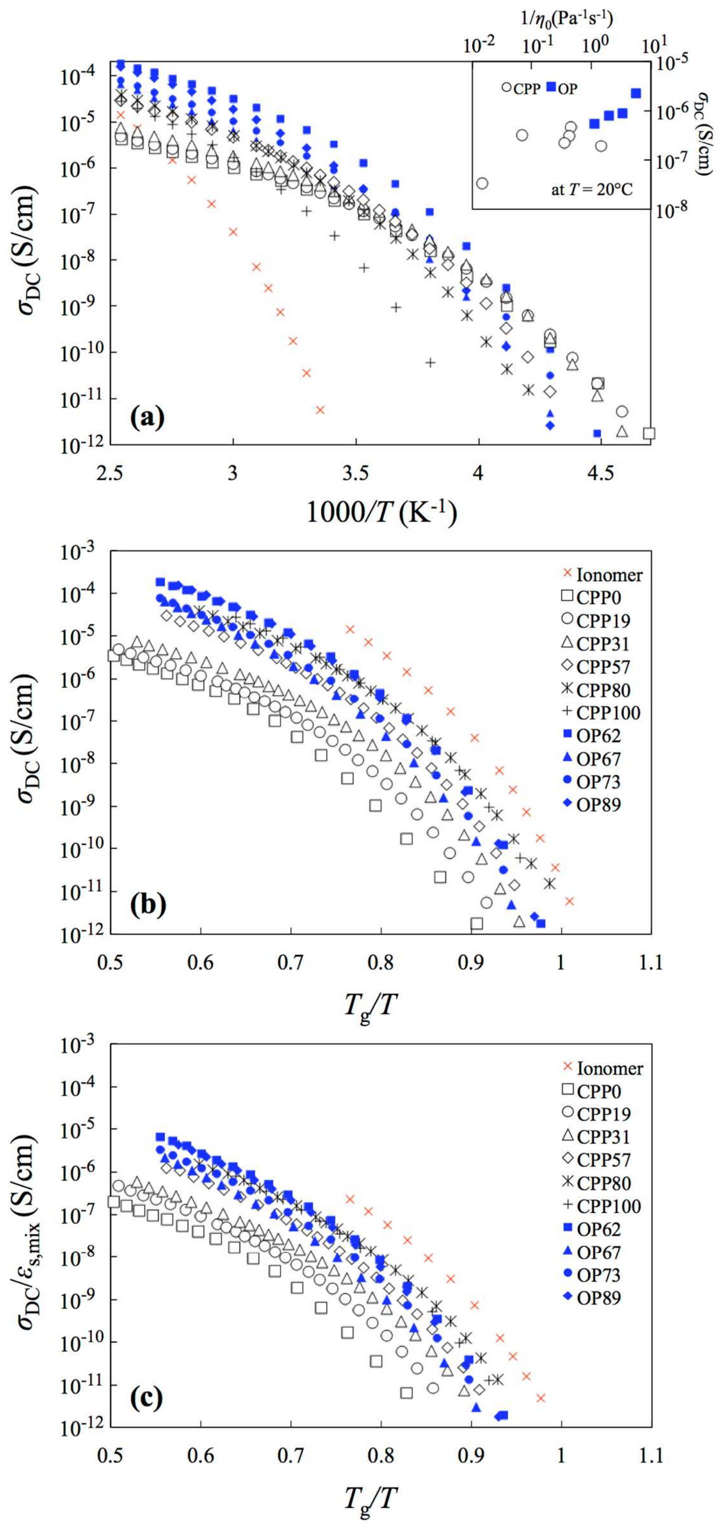

Figure 3. (a) Temperature dependence of ionic conductivity for the ionomer (red x symbols) and its blends with CPP (black symbols) and OP (blue symbols) at 20wt% ionomer. Inset: σ_{DC} versus $1/\eta_0$ at T = 20°C. (b) T_g/T dependence of the ionic conductivity. (c) T_g/T dependence of ionic conductivity divided by static dielectric constant.

Table 1. Molecular weight, T_g, and static dielectric constant ε_s and zero-shear viscosity η_0 of plasticizers measured at 20°C.

	CPP0	CPP19	CPP31	CPP57	CPP80	CPP100	OP62	OP67	OP73	OP89
M (g.mol^{-1})^a	12700	12400	12200	11800	11400	11100	626	651	695	450
T_g (K)	187	194	202	218	229	248	213	214	212	220
ε_S	5.9	11	15	27	38	54	37	24	29	48
η_0 (Pa s)	0.70	2.83	2.39	2.21	14.8	68.6	0.18	0.87	0.51	0.30

a: Number-average molecular weight, calculated from f, assuming number-average DP=52.

OP62 appears to be the best choice for plasticizer at any temperature above 250 K, of the ten samples studied here (see Figure 3a). This plasticizer is the only one with Si-O-C linkages, which are polar, flexible and easily hydrolyzed in the presence of moisture. OP62 has dielectric constant 30% larger than the Landau-Lifshitz prediction (see inset of Figure 2(b)), and by far the lowest viscosity (Table 1) even though T_g is only 10 K lower than the Fox equation (Figure 1).

Conclusions:

Two groups of low-volatility plasticizers are synthesized: both are composed of highly polar cyclic carbonate and short ethylene oxide chains. Those novel low-volatility plasticizers might replace organic carbonate solvent used in the lithium-ion battery industry to eliminate the safety problems existing in current rechargeable lithium-ion batteries. The combination of ethylene oxide and cyclic carbonate can tune T_g and dielectric constant to optimize σ_{DC}. The final performance of the plasticizers is decided by their chemical structure, consequently T_g, dielectric constant and viscosity. The best plasticizer OP62 has the lowest viscosity, the most flexible structure and nearly the highest dielectric constant. Polymer single-ion conductor blends containing those plasticizers and borate ionomer have room temperature conductivity up to 2 x 10^{-5} S/cm at 25 ºC. By mixing with low-volatility polar plasticizers, these ionomers are potential candidates to make safer gel polymer electrolytes for lithium-ion rechargeable battery separators.

Acknowledgments

The authors gratefully acknowledge the financial support of the Department of Energy under Grant BES-DE-FG02-07ER46409. Janna Maranas, Karl Mueller (both at Penn State) and Karen Winey from the University of Pennsylvania are thanked for helpful discussions.

Supporting Information available: Composition of copolymer plasticizers and NMR spectra of all plasticizers. This material is available free of charge via the Internet.

References

1. K. E. Thomas, S. E. Sloop, J. B. Kerr and J. Newman, *J Power Sources*, 2000, **89**, 132-138.
2. P. V. Wright, *MRS Bull*, 2002, **27**, 597-602.
3. D. Fragiadakis, S. Dou, R. H. Colby and J. Runt, *J Chem Phys*, 2009, **130,** 064907.
4. W. Wang, G. J. Tudryn, R. H. Colby and K. I. Winey, *J Am Chem Soc*, 2011, **133**, 10826-10831.
5. G. J. Tudryn, M. V. O'Reilly, S. C. Dou, D. R. King, K. I. Winey, J. Runt and R. H. Colby, *Macromolecules*, 2012, **45**, 3962-3973.
6. Q. Chen, H. Masser, H.-S. Shiau, S. Liang, J. Runt, P. C. Painter and R. H. Colby, *Macromolecules*, 2014, **47**, 3635-3644.
7. N. Matsumi, K. Sugai, K. Sakamoto, T. Mizumo and H. Ohno, *Macromolecules*, 2005, **38**, 4951-4954.
8. X. G. Sun and J. B. Kerr, *Macromolecules*, 2006, **39**, 362-372.
9. B. S. Qin, Z. H. Liu, G. L. Ding, Y. L. Duan, C. J. Zhang and G. L. Cui, *Electrochim Acta*, 2014, **141**, 167-172.
10. Y. S. Zhu, S. Y. Xiao, Y. Shi, Y. Q. Yang and Y. P. Wu, *Journal of Materials Chemistry A*, 2013, **1**, 7790-7797.
11. T. Fujinami, M. A. Mehta, K. Sugie and K. Mori, *Electrochim Acta*, 2000, **45**, 1181-1186.
12. W. Liu, M. J. Janik and R. H. Colby, in *Polymers for Energy Storage and Delivery: Polyelectrolytes for Batteries and Fuel Cells*, eds. K. A. Page, C. L. Soles and J. Runt, ACS Symp. Series, 2012, vol. 1096, ch. 2, pp. 19-44.
13. S. Liang, U. H. Choi, W. J. Liu, J. Runt and R. H. Colby, *Chemistry of Materials*, 2012, **24**, 2316-2323.
14. J. Y. Song, Y. Y. Wang and C. C. Wan, *J Power Sources*, 1999, **77**, 183-197.
15. A. M. Stephan, *Eur Polym J*, 2006, **42**, 21-42.
16. P. Zhang, L. L. Li, D. N. He, Y. P. Wu and M. Shimizu, *Acta Polym Sin*, 2011, 125-131.
17. M. Forsyth, J. Sun, F. Zhou and D. R. MacFarlane, *Electrochim Acta*, 2003, **48**, 2129-2136.
18. K.-D. Kreuer, A. Wohlfarth, C. C. de Araujo, A. Fuchs and J. Maier, *ChemPhysChem*, 2011, **12**, 2558–2560.
19. Y. V. Baskakova, O. V. Yarmolenko and O. N. Efimov, *Russian Chemical Reviews* 2012, **81**, 367-380.
20. J. R. MacCallum and C. A. Vincent, *Polymer Electrolyte Reviews*, Springer, 1987.
21. H.-S. Shiau, W. J. Liu, R. H. Colby and M. J. Janik, *J Chem Phys*, 2013, **139**, 204905.
22. U. H. Choi, S. Liang, M. V. O'Reilly, K. I. Winey, J. Runt and R. H. Colby, *Macromolecules*, 2014, **47**, 3145-3153.
23. D. K. Pradhan, R. N. P. Choudhary and B. K. Samantaray, *Mater Chem Phys*, 2009, **115**, 557-561.
24. Y. Ito, K. Kanehori, K. Miyauchi and T. Kudo, *J Mater Sci*, 1987, **22**, 1845-1849.
25. J. Y. Lee, Y. M. Lee, B. Bhattacharya, Y. C. Nho and J. K. Park, *J Solid State Electr*, 2010, **14**, 1445-1449.
26. F. Kaneko, S. Wada, M. Nakayama, M. Wakihara, J. Koki and S. Kuroki, *Adv Funct Mater*, 2009, **19**, 918-925.
27. Y. W. Li, J. W. Wang, J. W. Tang, Y. P. Liu and Y. D. He, *J Power Sources*, 2009, **187**, 305-311.
28. M. V. O'Reilly, H. Masser, D. R. King, P. P. C., R. H. Colby, K. I. Winey and J. Runt, *Polymer*, 2015, **59**, 133-143.
29. N. Tsukada and J. F. Hartwig, *J Am Chem Soc*, 2005, **127**, 5022-5023.
30. L. D. Landau and E. M. Lifshitz, *Electrodynamics of Continuous Media*, Oxford, Pergamon Press, 1963.
31. L. Onsager, *J Am Chem Soc*, 1936, **58**, 1486-1493.
32. Z. Zhang, D. Sherlock, R. West, R. West, K. Amine and L. J. Lyons, *Macromolecules*, 2003, **36**, 9176-9180.
33. Z. Zhang, L. J. Lyons, R. West, K. Amine and R. West, *Silicon Chemistry*, 2005, **3**, 259-266.
34. N. A. A. Rossi and R. West, *Polymer International*, 2009, **58**, 267–272.

35. B. Oh, R.C. West, K. Amine, US Patent 7,588,859. 2009.
36. P. Z. Walden, *Physik Chem*, 1906, **55**, 207-246.

Table of Contents (TOC) Graphic